Smart Mater. Struct. **20** (2011) 025009 (9pp) doi:10.1088/0964-1726/20/2/025009

Tailoring vibration mode shapes using topology optimization and functionally graded material concepts

Wilfredo Montealegre Rubio[1,5], **Glaucio H Paulino**[2,3] **and Emilio Carlos Nelli Silva**[4,5]

[1] School of Mechatronic of the Faculty of Mines, National University of Colombia, Carrera 80 No. 65-223, bloque M8, oficina 113, Medellín, Antioquia, Colombia
[2] Newmark Laboratory, Department of Civil and Environmental Engineering, University of Illinois at Urbana-Champaign, 205 North Mathews Avenue, Urbana, IL 61801, USA
[3] Department of Mechanical Science and Engineering, University of Illinois at Urbana-Champaign, 158 Mechanical Engineering Building, 1206 West Green Street, Urbana, IL 61801-2906, USA
[4] Department of Mechatronics and Mechanical Systems Engineering, Escola Politécnica da Universidade de São Paulo, Avenida Professor Mello Moraes, 2231-Cidade Universitária, São Paulo SP-05508-900, Brazil

E-mail: wmontealegrer@unal.edu.co and ecnsilva@usp.br

Received 6 August 2010, in final form 4 November 2010
Published 13 January 2011
Online at stacks.iop.org/SMS/20/025009

Abstract
Tailoring specified vibration modes is a requirement for designing piezoelectric devices aimed at dynamic-type applications. A technique for designing the shape of specified vibration modes is the topology optimization method (TOM) which finds an optimum material distribution inside a design domain to obtain a structure that vibrates according to specified eigenfrequencies and eigenmodes. Nevertheless, when the TOM is applied to dynamic problems, the well-known grayscale or intermediate material problem arises which can invalidate the post-processing of the optimal result. Thus, a more natural way for solving dynamic problems using TOM is to allow intermediate material values. This idea leads to the functionally graded material (FGM) concept. In fact, FGMs are materials whose properties and microstructure continuously change along a specific direction. Therefore, in this paper, an approach is presented for tailoring user-defined vibration modes, by applying the TOM and FGM concepts to design functionally graded piezoelectric transducers (FGPT) and non-piezoelectric structures (functionally graded structures—FGS) in order to achieve maximum and/or minimum vibration amplitudes at certain points of the structure, by simultaneously finding the topology and material gradation function. The optimization problem is solved by using sequential linear programming. Two-dimensional results are presented to illustrate the method.

(Some figures in this article are in colour only in the electronic version)

1. Introduction

Tailoring specified vibration modes is a requirement for designing resonators (Sanchez-Rojas *et al* 2010, Maeda *et al* 2006, Howe and Boser 1996), actuators (Jose *et al* 2002) and vibro-motors, which transform a mechanical vibration into a linear (Sharp *et al* 2010, Sun *et al* 2010, Saitou *et al* 2000, Pai and Tien 2000) or rotational (Lee and Pisano 1992) motion. On the other hand, considering a structure made of piezoelectric material, tailoring a specified vibration mode is advantageous for designing: (i) piezoelectric transducers for power applications such as sonotrodes (Or *et al* 2007);

[5] Authors to whom any correspondence should be addressed.

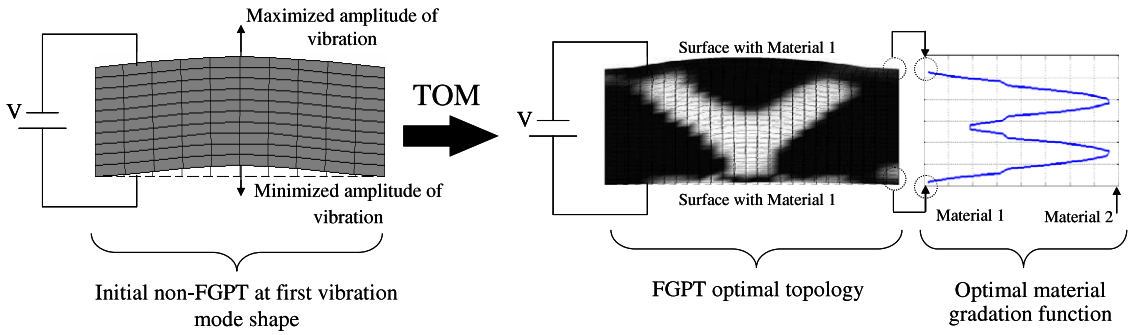

Figure 1. Sketch of the FGPT design by using the TOM, where the goal is to simultaneously find the topology and its material gradation function (when FGSs are considered, the voltage input excitation is replaced by concentrated mechanical load excitation).

(ii) ultrasonic transducers for medical and non-destructive testing (by tailoring the well-known piston-like mode) (Rubio *et al* 2009); and (iii) ultrasonic piezoelectric motors (Uchino and Giniewicz 2003).

A technique for designing the shape of specified vibration modes is the topology optimization method (TOM). Essentially, TOM finds a material distribution problem inside a design domain subjected to loads and boundary conditions, aiming, for example, to design a structure which vibrates according to specified eigenfrequencies and eigenmodes (Maeda *et al* 2006). Nevertheless, when TOM is applied to dynamic problems, the well-known grayscale or intermediate material problem arises, which can invalidate the post-processing of the optimal result (Bendsøe and Sigmund 2003).

An important issue to be addressed in the topology optimization is how to change the material density from zero (void) to one (solid material). The use of discrete values leads to ill-posedness due to multiple local minima and should therefore be avoided. However, the problem can be relaxed during the optimization by assuming intermediate densities, which is achieved by setting an appropriate continuous material model, where the formulation for intermediate materials (between 0 and 1) defines the level of problem relaxation. Nevertheless, at the end of the TOM (post-processing phase), the grayscale regions should be interpreted and approximated to bound values (zero or one), which modifies the final performance. As a result, there is a tradeoff between the final performance of the topology-optimized structure and its post-processed final topology, especially in dynamic applications. Accordingly, when material is added or removed during post-processing, the final eigenfrequencies and eigenvalues (mode shapes) are modified. For alleviating this problem, several options have been proposed such as filtering techniques (Bourdin 2001), the perimeter control method (Haber *et al* 1996) and the projection technique (Guest *et al* 2004). However, as shown by Maeda *et al* (2006), even using some of those schemes, the final topology will not be free of grayscales. Therefore, a more natural way for solving dynamic problems using TOM is to allow intermediate material values. This idea leads to the functional graded material (FGM) concept. FGMs are materials whose properties and microstructure continuously change along a specific direction (Aboudi *et al* 1999). By using the FGM concept and TOM, Rubio *et al* (2009) have tailored the piston-like mode of ultrasonic piezoelectric transducers; however, the work is limited to finding the optimal gradation function without considering the topological design.

In this work, an approach is presented for tailoring user-defined vibration modes by applying TOM and FGM concepts to design functionally graded piezoelectric transducers (FGPT) and non-piezoelectric structures (functionally graded structures—FGS) in order to achieve maximum and/or minimum vibration amplitudes at certain points of the structure (see figure 1), finding simultaneously the topology and material gradation function.

This work is arranged as follows. In section 2, FGPT and FGS modeling is presented and, in section 3, the topology optimization problem and its implementation are detailed. It is noteworthy that all the theoretical formulations will be presented considering the focus on FGPT, as the FGS problem is a simplification of the former. Finally, in sections 4 and 5, numerical results are presented and conclusions are inferred, respectively.

2. FGPT and FGS finite element modeling

By using a modal analysis, the natural frequencies and vibration mode shapes are obtained. Specifically, in a piezoelectric analysis, the following eigenvalue and eigenvector problem is solved (damping effects are not considered) (Lerch 1990):

$$-\lambda \begin{bmatrix} \mathbf{M_{uu}} & 0 \\ 0 & 0 \end{bmatrix} \begin{Bmatrix} \mathbf{\Psi_u} \\ \mathbf{\Psi}_\varphi \end{Bmatrix} + \begin{bmatrix} \mathbf{K_{uu}} & \mathbf{K}_{\mathbf{u}\varphi} \\ \mathbf{K}_{\mathbf{u}\varphi}^{\mathrm{T}} & -\mathbf{K}_{\varphi\varphi} \end{bmatrix} \begin{Bmatrix} \mathbf{\Psi_u} \\ \mathbf{\Psi}_\varphi \end{Bmatrix} = \begin{Bmatrix} \mathbf{0} \\ \mathbf{0} \end{Bmatrix} \qquad \text{with: } \lambda = \omega^2 \tag{1}$$

where

$$\mathbf{M_{uu}} = \sum_{e=1}^{nel} \int\int\int_{\Omega_e} \mathbf{N}_\mathbf{u}^{\mathrm{T}} \rho(x, y, z) \mathbf{N_u} \, \mathrm{d}x \, \mathrm{d}y \, \mathrm{d}z; \tag{2}$$

$$\mathbf{K_{uu}} = \sum_{e=1}^{nel} \int\int\int_{\Omega_e} \mathbf{B_u^T} c^{\mathrm{E}}(x, y, z)\mathbf{B_u}\, \mathrm{d}x\, \mathrm{d}y\, \mathrm{d}z;$$

$$\mathbf{K_{u\varphi}} = \sum_{e=1}^{nel} \int\int\int_{\Omega_e} \mathbf{B_u^T} e^{\mathrm{T}}(x, y, z)\mathbf{B}_\varphi\, \mathrm{d}x\, \mathrm{d}y\, \mathrm{d}z; \qquad (3)$$

$$\mathbf{K}_{\varphi\varphi} = \sum_{e=1}^{nel} \int\int\int_{\Omega_e} \mathbf{B}_\varphi^{\mathrm{T}} \boldsymbol{\varepsilon}^{\mathrm{S}}(x, y, z)\mathbf{B}_\varphi\, \mathrm{d}x\, \mathrm{d}y\, \mathrm{d}z;$$

where the term c^{E} is the elastic property matrix (elastic stiffness at constant electric field); $\boldsymbol{\varepsilon}^{\mathrm{S}}$ is the dielectric property matrix (dielectric susceptibility at constant strain); the term e is the piezoelectric property matrix; and ρ is the material density. All properties depend on Cartesian coordinates x, y and z. Additionally, the terms $\mathbf{M_{uu}}$, $\mathbf{K_{uu}}$, $\mathbf{K_{u\varphi}}$ and $\mathbf{K}_{\varphi\varphi}$ are the mass, stiffness, piezoelectric and dielectric global matrices, respectively. According to finite element theory, global matrices are formed for each finite element e contribution (being represented by the summation symbol in equations (2) and (3)). The eigenvalue and natural frequency are represented by the terms λ and ω, respectively, and $\boldsymbol{\Psi} = \{\, \boldsymbol{\Psi}_{\mathbf{u}} \quad \boldsymbol{\Psi}_\varphi \,\}^{\mathrm{T}}$ is the eigenvector. Finally, the superscript T indicates transpose; the constant *nel* represents the total number of finite elements used for discretization; the term $\mathbf{N_u}$ are the shape functions, and $\mathbf{B_u}$ and $\mathbf{B}_\varphi$ are the strain–displacement and voltage-gradient matrices. Equation (1) has been reduced by considering the short-circuited electrodes; that is, the electrical potential in the electrodes has been set to zero in equation (1).

It is observed from equations (2) and (3) that material properties depend on the Cartesian position (x, y and z), according to the FGM concept. In numerical implementation, the change in material properties is considered by using the graded finite element (GFE) concept (Kim and Paulino 2002), where the properties are interpolated inside each finite element e based on nodal property values. In this research, the same shape functions for interpolating geometry and displacements are used for material property interpolation. For FGPT, the GFE concept yields

$$\rho(x, y, z) = \sum_{m=1}^{n} N_m(x, y, z)\rho_m,$$

$$c^{\mathrm{E}}_{ijkl}(x, y, z) = \sum_{m=1}^{n} N_m(x, y, z)(c^{\mathrm{E}}_{ijkl})_m,$$

$$e_{ikl}(x, y, z) = \sum_{m=1}^{n} N_m(x, y, z)(e_{ikl})_m,$$

$$\varepsilon^{\mathrm{S}}_{ik}(x, y, z) = \sum_{m=1}^{n} N_m(x, y, z)(\varepsilon^{\mathrm{S}}_{ik})_m \qquad \text{for } i, j, k, l = 1,2,3 \qquad (4)$$

where ρ, c^{E}_{ijkl}, e_{ikl} and $\varepsilon^{\mathrm{S}}_{ik}$ represent density, elastic, piezoelectric and dielectric material properties, respectively. The term n is the number of nodes per finite element. Further details of the GFE concept can be found in Kim and Paulino (2002) and Silva *et al* (2007).

Finally, as observed in equation (1), the FGS modeling is a simplification of the more general FGPT one; in other words, the electric and piezoelectric effects are neglected. Hence, for FGS, the modal analysis can be expressed as

$$-\lambda\mathbf{M_{uu}}\boldsymbol{\Psi_u} + \bar{\mathbf{K}}_{\mathbf{uu}}\boldsymbol{\Psi_u} = 0 \qquad \text{with :}$$

$$\bar{\mathbf{K}}_{\mathbf{uu}} = \sum_{e=1}^{nel} \int\int\int_{\Omega_e} \mathbf{B_u^T}\mathbf{E}(x, y, z)\mathbf{B_u}\, \mathrm{d}x\, \mathrm{d}y\, \mathrm{d}z; \qquad (5)$$

where $\mathbf{E}$ represents the elastic matrix for a non-piezoelectric material.

3. Topology optimization applied to FGPT and FGS design

3.1. Material model

In this work, the material at each point inside the design domain is defined by using a combination between two 'traditional' material models: (i) the rational approximation of material properties (RAMP) (Pedersen 2000) and (ii) the solid isotropic material with penalization (SIMP) (Bendsøe and Sigmund 2003). This combination of models is formulated due to the fact that in the dynamic analysis of structures the use of SIMP only causes local vibration modes in regions where the design variables have a low value (Neves *et al* 1995); specifically, localized modes appear in areas where the design variables have the minimum admissible value (usually near to zero: 10^{-3}). These areas are more flexible in relation to areas with high design variable values and, consequently, they control the lower-order modes (Pedersen 2000). Thus, if a material model based on a power-law function with an improper combination of exponents is chosen, the problem of localized eigenmodes is likely to arise. For instance, by adopting the SIMP material model with penalizations equal to 3 and 1 for the stiffness and mass properties, respectively, the ratio between mass and stiffness tends to infinite values when the design variable tends to 0, which causes the appearance of eigenvalues associated with localized modes, specifically, related to the lowest modes (Pedersen 2000). For overcoming this problem, Stolpe and Svanberg (2001), Bendsøe and Sigmund (2003) and Hansen (2005) proposed an alternative by defining RAMP and SIMP material models for elastic and density properties, respectively.

The material model for elastic properties is given by (Stolpe and Svanberg 2001)

$$C^H(x, y) = C_3 + \left[\frac{\rho_{1_{\mathrm{TOM}}}(x, y)}{1 + p_1(1 - \rho_{1_{\mathrm{TOM}}}(x, y))}\right] \times [(\rho_{2_{\mathrm{TOM}}}(x, y)C_1 + (1 - \rho_{2_{\mathrm{TOM}}}(x, y))C_2) - C_3] \qquad (6)$$

where the design variable $\rho_{1_{\mathrm{TOM}}}(x, y)$ controls the topology of the structure (see figure 2); in other words, it controls the amount of FGM inside the design domain. The design variable $\rho_{2_{\mathrm{TOM}}}(x, y)$ defines the composition of the graded material, that is, it determines the FGM obtained by mixing two base materials (non-graded materials) type j ($j = 1, 2, 3$), see figure 2. On the other hand, the term p_1 is a penalization term for intermediate design variables $\rho_{1_{\mathrm{TOM}}}(x, y)$, typically chosen larger than three; the term C_i ($i = 1, 2, 3$) defines the elastic properties coefficients where,

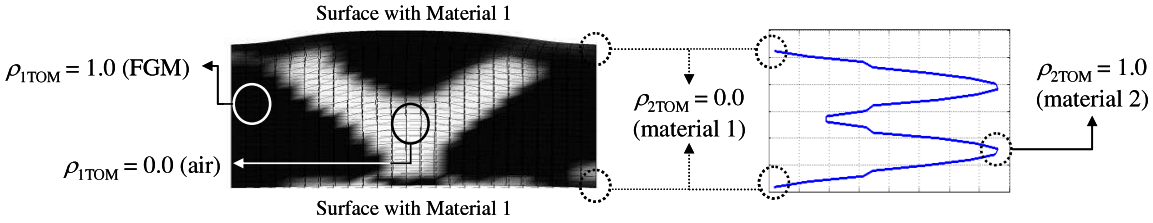

Figure 2. Sketch of material model schemes for FGPT or FGS design.

for the FGPT design, the value $i = 1$ indicates piezoelectric material, $i = 2$ depicts piezoelectric or non-piezoelectric material and $i = 3$ represents air. For FGS design, materials type 1 and type 2 are non-piezoelectric materials. Finally, C^H is the 'mixed' FGM elastic properties. Specifically, the considered optimization problem aims to perform a 0–1 material distribution represented by air (0) and solid FGM material (1), where the FGM material is composed of two materials: type 1 and type 2; that is, we are digging holes in an FGM material and at the same time finding its optimal gradation. However, the material model allows intermediate values (mixtures) of material type 1 and type 2.

On the other hand, for density, piezoelectric and dielectric properties, the material model is formulated based on the SIMP one, which is defined as follows:

$$D^H(x, y) = \rho_{1_{\mathrm{TOM}}}^{p_2}(\rho_{2_{\mathrm{TOM}}}(x, y)D_1 + (1 - \rho_{2_{\mathrm{TOM}}}(x, y))D_2) - (1 - \rho_{1_{\mathrm{TOM}}}^{p_2}(x, y))D_3 \tag{7}$$

where p_2 is a penalization power on design variables $\rho_{1_{\mathrm{TOM}}}$, the term D^H refers to the density, dielectric or piezoelectric properties of the FGM and the constants D_i are the density, dielectric or piezoelectric properties for each base material type i ($i = 1, 2, 3$).

Figure 2 illustrates an example of the result that can be obtained through this formulation. The white region, represented by $\rho_{1_{\mathrm{TOM}}} = 0.0$, corresponds to air and the black region, represented by $\rho_{1_{\mathrm{TOM}}} = 1.0$, corresponds to FGM material. The FGM material considered in this work has a horizontal layer-type gradation which will also be optimized. The plot on the right shows the final optimized gradation distribution. Thus, for all properties, when $\rho_{1_{\mathrm{TOM}}} = 1.0$ or $\rho_{1_{\mathrm{TOM}}} = 0.0$, FGM or air properties are obtained, respectively (see figure 2). On the other hand, $\rho_{2_{\mathrm{TOM}}} = 1.0$ denotes properties of the material type 1 and $\rho_{2_{\mathrm{TOM}}} = 0.0$ represents properties of the material type 2 inside FGM (see figure 2).

3.2. Optimization problem formulation

The design objective, both FGPT and FGS, is formulated in order to find, by using the TOM, the topology and material gradation law, which maximizes and/or minimizes the vibration amplitude in specified points of the structure, when the structure vibrates at the desirable mode k. Figure 1 shows these problem specifications. In the same way, by maximizing and/or minimizing specified vibration amplitudes, the vibration mode shape of the mode k can be tailored.

The proposed optimization problem based on multi-objective function is formulated in its discrete form as

$$\underset{\rho_{1_{\mathrm{TOM}_i}}, \rho_{2_{\mathrm{TOM}_i}}}{\text{maximize}} \; F = w_1\left[\sum_{k=1}^{m_1} w_{2k}\log((\boldsymbol{t}_{k_{\max}}^{\mathrm{T}}\boldsymbol{\Psi}_{r_k})^2) - \sum_{k=1}^{m_2} w_{3k}\log((\boldsymbol{t}_{k_{\min}}^{\mathrm{T}}\boldsymbol{\Psi}_{r_k})^2)\right] - (1 - w_1)\sum_{k=1}^{m_1+m_2} w_{4k}\log(L_{33_k}^2)$$

such that:

$$\sum_{i=1}^{N_{\mathrm{des}}} \rho_{1_{\mathrm{TOM}_i}} V_i - V_{s_1}^* \leqslant 0$$

$$\sum_{i=1}^{N_{\mathrm{des}}} \rho_{2_{\mathrm{TOM}_i}} V_i - V_{s_2}^* \leqslant 0$$

$$0 \leqslant \rho_{1_{\mathrm{TOM}_i}} \leqslant 1 \qquad \text{for } i = 1, \ldots, N_{\mathrm{des}}$$

$$0 \leqslant \rho_{2_{\mathrm{TOM}_i}} \leqslant 1 \qquad \text{for } i = 1, \ldots, N_{\mathrm{des}}$$

equilibrium equations (*see either equation* (*1*) *or* (*4*), *according to problem*). (8)

In relation to objective function F, the terms m_1 and m_2 are the number of modes whose amplitude of vibration must be maximized and/or minimized, respectively. The vector $\boldsymbol{\Psi}_{\mathrm{r}}$ represents the resonance eigenvector of the mode number k, and the terms $\boldsymbol{t}_{k_{\max}}$ and $\boldsymbol{t}_{k_{\min}}$ are respectively dummy vectors, which are vectors consisting of zeros except for the position corresponding to the d.o.f that must be maximized or minimized where it has a value equal to one, for each corresponding mode k. Finally, the constants w_i ($i = 1, \ldots, 4$) are weight coefficients for each goal. Nevertheless, if only the first two terms are maximized (aiming to maximize the amplitude of vibration at specific points of the mode k), the formulation would lead to very low stiffness results. This problem is well known from the design of compliant mechanisms (Sigmund 1997). Hence, the term L_{33_k} is added to the objective function (see equations (8)), which represents the mean compliance for achieving static stiffness (Maeda *et al* 2006, Silva *et al* 2000, Nishiwaki *et al* 1998).

On the other hand, terms $\rho_{1_{\mathrm{TOM}_i}}$ and $\rho_{2_{\mathrm{TOM}_i}}$ represent the design variables at node i ($i = 1, 2, 3, \ldots, N_{\mathrm{des}}$), according to the continuous approximation of material distribution (CAMD) scheme (Matsui and Terada 2004). The value V_i is the quantity of FGM at node i ($i = 1, 2, 3, \ldots, N_{\mathrm{des}}$). Terms $V_{s_1}^*$ and $V_{s_2}^*$ represent FGM and material type 1 constraints, respectively. The constant N_{des} denotes the total number of nodes. The two

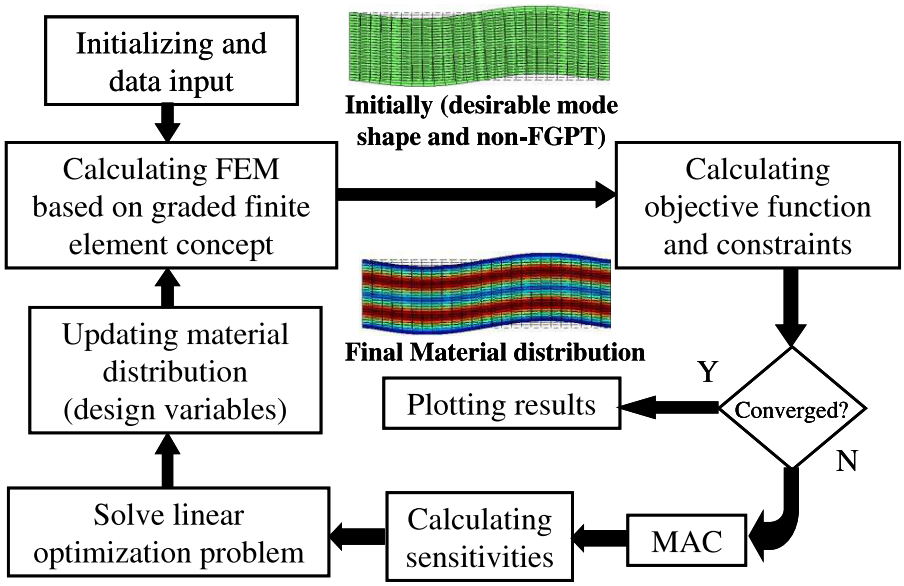

Figure 3. Flowchart of the topology optimization implementation.

constraint values related to design variables $\rho_{1_{\mathrm{TOM}_i}}$ and $\rho_{2_{\mathrm{TOM}_i}}$ seem to have a strong influence when designing to achieve specified eigenvalues (resonance frequencies). However, since the optimization problem considers the vibration mode design only (maximizing vibration amplitudes at specified points), these constraint values do not seem to have such a strong influence in the final result.

Finally, the topology optimization problem for the $\rho_{2_{\mathrm{TOM}_i}}$ design variable is formulated as a layer-like optimization problem, aimed at sintering the designed components as a layer-structured green piece without any adhesive material; hence, the design variables $\rho_{2_{\mathrm{TOM}_i}}$ are considered equal at each layer, as shown in Rubio *et al* (2009).

3.3. Numerical implementation

The numerical procedure follows the implementation shown in Rubio *et al* (2009). Four numerical techniques are used for implementing our approach (Rubio *et al* 2009): (i) firstly, the GFE concept (Kim and Paulino 2002) is utilized for simulating the continuous material gradation inside each finite element. (ii) Secondly, the CAMD (Matsui and Terada 2004) is used for assuming a continuous change of design variables. (iii) Thirdly, the projection technique (Guest *et al* 2004) is implemented for obtaining explicit control of the material gradient and, consequently, for obtaining a smooth gradation function, which represents a smooth change of properties along the gradation direction. Finally, (iv) the modal assurance criterion (MAC) (Kim and Kim 2000) is adopted to follow the desirable vibration mode shape along the iterative process of the TOM (see figure 3). Specifically, the MAC compares pairs of vibration modes and gives their correlation level to find the desired mode (Kim and Kim 2000).

Figure 3 shows a flowchart of the optimization algorithm. First of all, the initial domain is discretized by graded finite elements and the design variables are defined at each node. The proposed formulation is implemented by using Matlab™ code. The Q4/Q4 graded finite element (Rahmatalla and Swan 2004) is used, which represents a two-dimensional four-node quadrilateral GFE. For FGPT design, each node has three degrees of freedom: two mechanical (horizontal and vertical displacements), and one electric (electrical potential) and, for FGS design, each node has two displacement degrees of freedom. Besides, each node has two design variables. In this research, the sequential linear programming method (SLP) is applied to solve the nonlinear optimization problem (Haftka *et al* 1990). It consists of the sequential solution of approximated linear sub-problems that can be defined by writing a Taylor series expansion for the nonlinear optimization problem around the current design point at each iteration step. This linearization requires the sensitivities (gradients) of the objective function and constraints in relation to each design variable set ($\rho_{1_{\mathrm{TOM}_i}}$ and $\rho_{2_{\mathrm{TOM}_i}}$). The sensitivity calculation is similar to that presented in Rubio *et al* (2009), with the additional complexity that each node has two design variables: terms $\rho_{1_{\mathrm{TOM}_i}}$ and $\rho_{2_{\mathrm{TOM}_i}}$.

Additionally, at each iteration, moving limits are defined for design variables ($\rho_{1_{\mathrm{TOM}_i}}$ and $\rho_{2_{\mathrm{TOM}_i}}$). During the iterative process, the design variables will be allowed to change by 5–15% of the original values. After linear optimization, a new set of design variables are obtained and updated in the design domain until convergence is achieved for the objective function. The procedure converges when the changes in design variables from iteration to iteration are below 10^{-3}.

4. Results

4.1. Design of an FGS

To illustrate the proposed method, first, a two-dimensional FGS is designed considering a plane strain assumption. The design domain used is shown in figure 4(a). The design

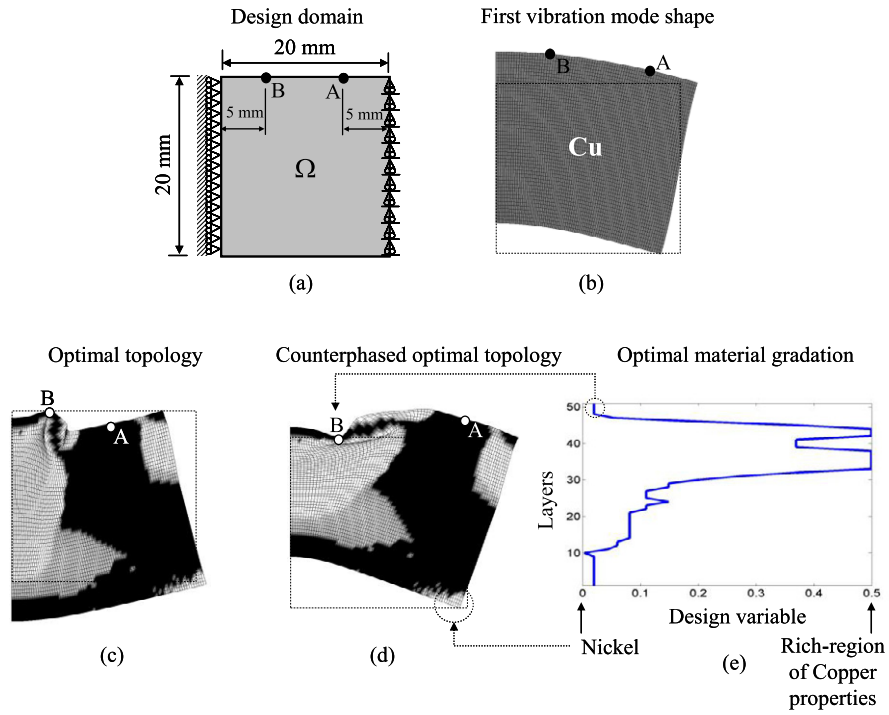

Figure 4. Design of an FGS by using TOM: (a) design domain; (b) initial first vibration mode (the dashed line represents undeformed domain); (c) final optimal topology (the dashed line represents undeformed domain); (d) counterphased optimal topology (the dashed line represents undeformed domain) and (e) final material gradation function.

Table 1. Parameters used in TOM.

Data	Design of an FGPT	Design of an FGS
Radius used in projection technique ($r_{\min}$)	2.5	3.5
FGM constraint function value, $V^*_{s_1}$	30	30
Initial values of $\rho_{1_{\text{TOM}}}$ and $\rho_{2_{\text{TOM}}}$	1	1
Number of smallest eigenvalues to be computed in FE analysis	50	60
Initial values for all penalization coefficients	1	1
Final value for penalization coefficient p_1	3	3
Final value for penalization coefficient p_2	1	—
- For piezoelectric properties	3	—
- For dielectric properties	1	—
- For density	1	1
Weight coefficient w_1	0.8	0.85
Weight coefficient w_2	1	1
Weight coefficient w_3	1	1
Weight coefficient w_4	1.5	1.5

domain is specified as 20 mm × 20 mm with mechanical boundary conditions as specified in figure 4(a). The idea is simultaneously to distribute three types of materials into the design domain. Material type 1 is represented by copper ($\rho_{2_{\text{TOM}}} = 1$), material type 2 by nickel ($\rho_{2_{\text{TOM}}} = 0$) and material type 3 by air. A material gradation along the thickness direction is assumed and a mesh of 80×50 finite elements is adopted. At each iteration, during the TOM procedure, 60 eigenmodes are calculated. For all results, the parameters used during topology optimization are defined in table 1. All material property values used are described in table 2.

The goal is to maximize the amplitude of vibration at point A and simultaneously to minimize the amplitude of vibration at point B; both requirements are defined for the first vibration mode when the design domain contains only copper (see figure 4(b)).

Figures 4(d) and (e) show the optimal topology and material gradation function after the topology optimization process. From the deformed topology (see figures 4(c) and (d)), it is observed that, at the first vibration mode, the vertical amplitude of vibration is maximized at point A and, simultaneously, is minimized at point B; accordingly, the initial goals are achieved. In addition, the first vibration frequency changes from 5.11 to 3.66 kHz.

These results can be confirmed by observing the convergence data in figures 5(a) and (b) for the desirable amplitudes of vibration. From these curves, it is clear that the relative amplitude at point A and B is incremented and reduced along the iterative process, respectively. In addition, the curves in figure 5 show oscillations at the end of the convergence process due to the fact that there is eigenmode switching during the iterative optimization. This switching appears frequently in applications of topology optimization to eigenproblems (Ma *et al* 1995, Rubio *et al* 2009), which arises due to fact that the order of the desirable eigenmode changes during the optimization. However, as the MAC has been implemented in this work, the target mode shape is always tracked at each iteration.

Finally, the material gradation function depicts an FGS with a rich region of nickel properties on the bottom and top surfaces, and a structure with approximately 50% nickel and 50% copper around layer numbers 30 and 45—see figure 4(e).

Table 2. Material properties.

Properties		PZT-5A	Copper	Nickel
Dielectric properties ($F\,m^{-1}$)	ε_0	8.85×10^{-12}	—	—
	ε_{11}^S	$916 \times \varepsilon_0$	—	—
	ε_{33}^S	$830 \times \varepsilon_0$	—	—
Piezoelectric properties ($C\,m^{-2}$)	e_{31}	−5.4	—	—
	e_{33}	15.8	—	—
	e_{15}	12.3	—	—
Elastic properties ($N\,m^{-2}$)	c_{11}^E	12.1×10^{10}	—	—
	c_{12}^E	7.54×10^{10}	—	—
	c_{13}^E	7.52×10^{10}	—	—
	c_{33}^E	11.1×10^{10}	—	—
	c_{44}^E	2.11×10^{10}	—	—
	c_{66}^E	2.28×10^{10}	—	—
	E (Young's modulus) (GPa)	—	115	200
	ν (Poisson's coefficient)	—	0.34	0.31
Density ($kg\,m^{-3}$)		7800	8940	8908

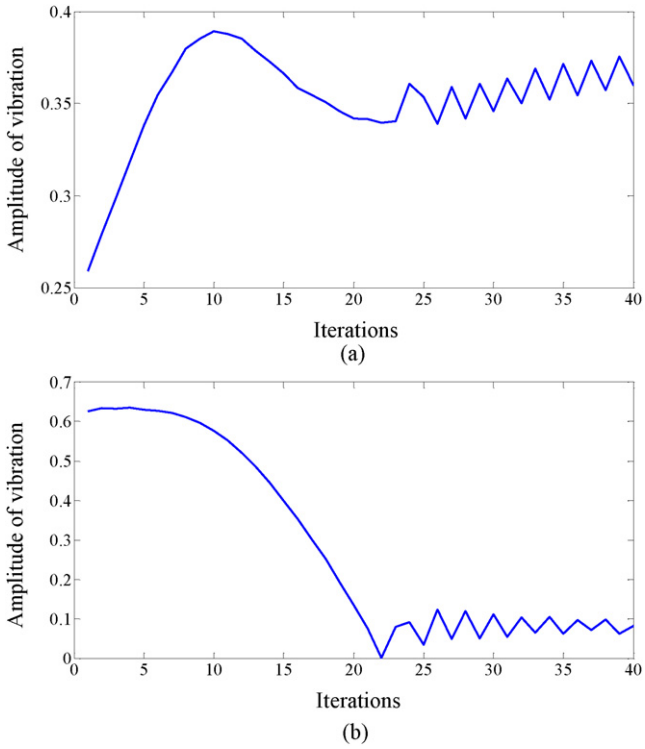

Figure 5. Convergence curves for: (a) relative amplitude of vibration at point A of figure 4(d) and (b) amplitude of vibration at point B of figure 4(d).

4.2. Design of an FGPT

In relation to FGPT design, the objective function F is maximized, see equation (8). In this case, the design domain of figure 6(a) is used and materials PZT-5A (material type 1), epoxy resin (material type 2) and air (material type 3) are combined. The main goal is to maximize the relative amplitude of vibration at point A and to minimize the amplitude of vibration at point B (see figure 6(b)). Both requirements are defined for vibration mode number 1 ($k = 1$). In figure 6, the applied voltage is sketched only for indicating the electrode position, as during modal analysis, no electrical potential is applied. The first mode is shown in figure 6(b), which is defined considering only a non-graded piezoelectric transducer with properties of PZT-5A. The design domain is discretized with 80×50 finite elements.

Figures 6(d) and (e) show the final topology and material distribution function after the optimization process. From the deformed structure (see figures 6(c) and (d)), it is observed that in fact the relative amplitude of vibration at point A is maximized and at point B is significantly minimized and, hence, the initial goals are satisfied. On the other hand, from figure 7, the historic convergence curve of the vibration amplitude of the above defined points is observed. Figure 7 confirms the results of figure 6. In this problem, the first vibration frequency varies from 49.45 to 16.34 kHz.

Finally, the material gradation represents a piezoelectric transducer with a rich region of epoxy resin near to the middle of the structure and a rich region of piezoelectric material (PZT-5A) on the bottom of the transducer (see figure 6(e)).

5. Conclusion

This paper presents a systematic study for designing piezoelectric and non-piezoelectric structures aimed at tailoring a specific vibration mode based on the topology optimization method and functionally graded material concept. The TOM design for dynamic problems, considering the FGM concept, seems to be more promising because it circumvents the post-processing problem related to the grayscale removal in traditional dynamic TOM problems. On the other hand, by using the TOM and the FGM concept, the optimal gradation and topology of FGPTs and FGSs can be found. Specifically, user-defined eigenvectors can be tailored aimed to design mechanical and piezoelectric resonators. Finally, examples of both FGPT and FGS demonstrate that the optimal topology

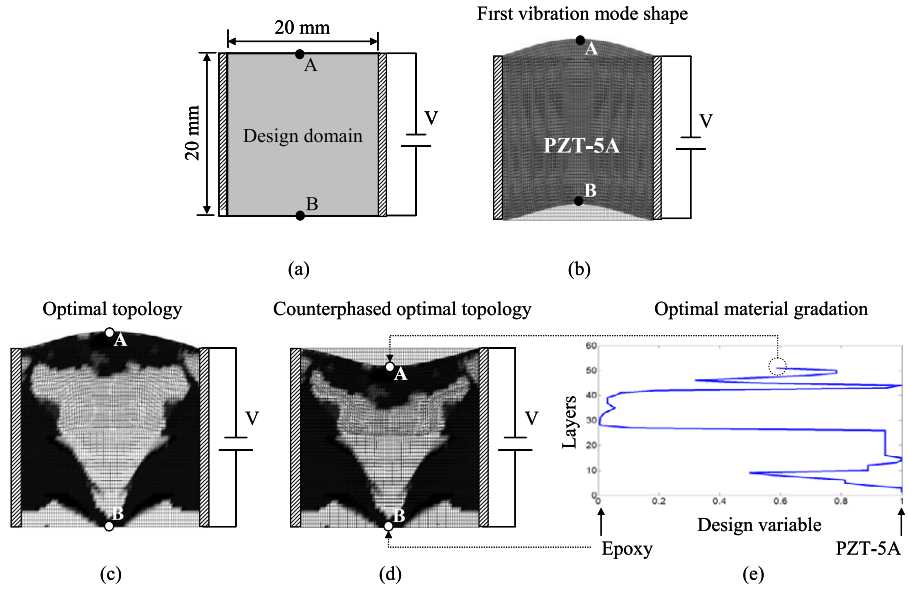

Figure 6. Design of an FGPT by using TOM: (a) design domain; (b) initial first vibration mode; (c) final optimal topology; (d) counterphased optimal topology; and (e) final material gradation function.

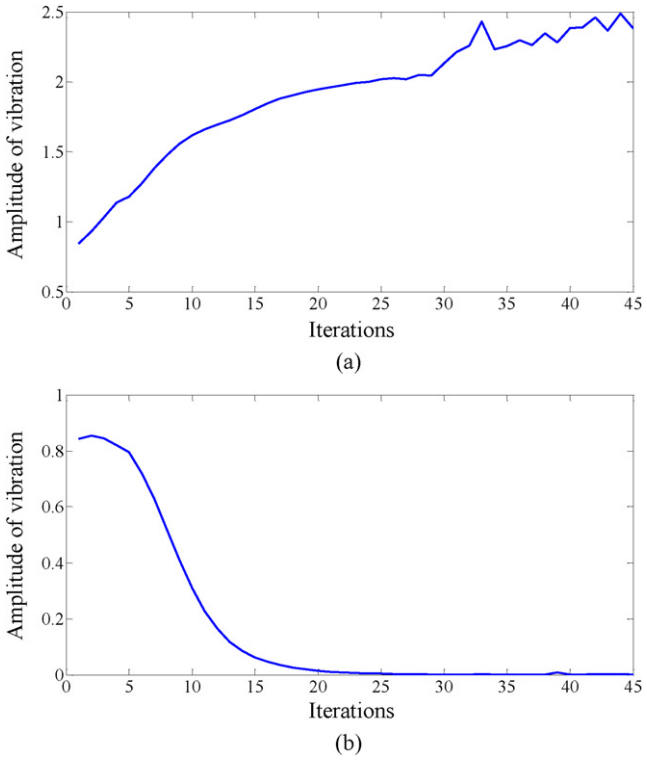

Figure 7. Convergence curves for: (a) relative amplitude of vibration at point A of figure 6(d) and (b) amplitude of vibration at point B of figure 6(d).

and material gradation can produce vibrating structures that have design-specified mode shapes; hence, by applying the proposed approach, the range of application of FGPTs and FGSs can be broadened and their design can become more systematic and generic.

Acknowledgments

The first author thanks FAPESP (São Paulo State Foundation Research Agency) for supporting him during his graduate studies through fellowship no. 05/01762-5. The second author also thanks FAPESP for a visiting professor grant (no. 08/51070-0) at the Polytechnic School of University of São Paulo (Brazil) during the second semester of 2008. The last author is grateful for the financial support received from both CNPq (National Council for Research and Development, Brazil, project no. 303689/2009-9) and FAPESP.

References

Aboudi J, Pindera M J and Arnold S M 1999 Higher-order theory for functionally graded materials *Composites* B **30** 777–832

Bendsøe M P and Sigmund O 2003 *Topology Optimization: Theory, Methods and Applications* (Berlin: Springer)

Bourdin B 2001 Filters in topology optimization *Int. J. Numer. Methods Eng.* **50** 2143–58

Guest J M, Prevost J H and Belytschko 2004 Achieving minimum length scale in topology optimization using nodal design variables and projection functions *Int. J. Numer. Methods Eng.* **61** 238–54

Haber R B, Jog C S and Bendsøe M P 1996 A new approach to variable-topology shape design using a constraint on parameter *Struct. Opt.* **11** 1–12

Haftka R T, Gürdal Z and Kamat M P 1990 *Element of Structural Optimization* (Dordrecht: Kluwer Academic)

Hansen L V 2005 Topology optimization of free vibrations of fiber laser packages *Struct. Multidiscip. Opt.* **29** 341–8

Howe R T and Boser B E 1996 Surface micromachined accelerometers *IEEE J. Solid-State Circuits* **31** 366–75

Jose K A, Suh W D, Xavier P B, Varadan V K and Varadan V V 2002 Surface acoustic wave MEMS gyroscope *Wave Motion* **36** 367–81

Kim J H and Paulino G H 2002 Isoparametric graded finite elements for nonhomogeneous isotropic and orthotropic materials *Trans. ASME J. Appl. Mech.* **69** 502–14

Kim T S and Kim Y Y 2000 MAC-based mode-tracking in structural topology optimization *Comput. Struct.* **74** 375–83

Lee A P and Pisano A P 1992 Polysilicon angular microvibromotors *J. Microelectromech. Syst.* **1** 621–9

Lerch R 1990 Simulation of piezoelectric devices by two- and three-dimensional finite elements *IEEE Trans. Ultrason. Ferroelectr. Freq. Control* **37** 233–47

Ma Z D, Kikuchi N and Cheng H C 1995 Topology design for vibration structures *Comput. Methods Appl. Mech. Eng.* **121** 259–80

Maeda Y, Nishiwaki S, Izui K, Yoshimura M, Matsui K and Terada K 2006 Structural topology optimization of vibrating structures with specified eigenfrequencies and eigenmode shapes *Int. J. Numer. Methods Eng.* **67** 597–628

Matsui K and Terada K 2004 Continuous approximation of material distribution for topology optimization *Int. J. Numer. Methods Eng.* **59** 1925–44

Neves M M, Rodrigues H and Guedes J M 1995 Generalized topology design of structures with a buckling load criterion *Struct. Opt.* **10** 71–8

Nishiwaki S, Frecker M I, Min S and Kikuchi N 1998 Topology optimization of compliant mechanisms using the homogenization method *Int. J. Numer. Methods Eng.* **42** 535–59

Or S W, Chan H L W and Liu P C K 2007 Piezocomposite ultrasonic transducer for high-frequency wire-bonding of microelectronics devices *Sensors Actuators* A **133** 195–9

Pai M and Tien N C 2000 Low voltage electomechanical vibromotor for silicon optical bench applications *Sensors Actuators* A **83** 237–43

Pedersen N L 2000 Maximization of eigenvalues using topology optimization *Struct. Multidiscip. Opt.* **20** 2–11

Rahmatalla S F and Swan C C 2004 A Q4/Q4 continuum structural topology optimization implementation *Struct. Multidiscip. Opt.* **27** 130–5

Rubio W M, Silva E C N and Paulino G H 2009 Toward optimal design of piezoelectric transducers based on multifunctional and smoothly graded hybrid material systems *J. Intell. Mater. Syst. Struct.* **20** 1725–46

Saitou K, Wang D-A and Wou S J 2000 Externally resonated linear microvibromotor for microassembly *J. Microelectromech. Syst.* **9** 336–46

Sanchez-Rojas J L, Hernando J, Donoso A, Bellido J C, Manzaneque T, Ababneh A, Seidel H and Schmid U 2010 Modal optimization and filtering in piezoelectric microplate resonators *J. Micromech. Microeng.* **20** 055027

Sharp S L, Paine J S N and Blotter J D 2010 Design of a linear ultrasonic piezoelectric motor *J. Intell. Mater. Syst. Struct.* **21** 961–73

Sigmund O 1997 On the design of compliant mechanisms using topology optimization *Mech. Struct. Mach.* **25** 493–524

Silva E C N, Carbonari R C and Paulino G H 2007 On graded elements for multiphysics applications *Smart Mater. Struct.* **16** 2408–28

Silva E C N, Nishiwaki S and Kikuchi N 2000 Topology optimization design of flextensional actuators *IEEE Trans. Ultrason. Ferroelectr. Freq. Control* **47** 657–71

Stolpe M and Svanberg K 2001 An alternative interpolation scheme for minimum compliance topology optimization *Struct. Multidiscip. Opt.* **22** 116–24

Sun D, Wang S, Sakurai J, Choi K-B, Shimokohbe A and Hata S 2010 A piezoelectric linear ultrasonic motor with the structure of a circular cylindrical stator and slider *Smart Mater. Struct.* **19** 045008

Uchino K and Giniewicz J R 2003 *Micromechatronics* (New York: Dekker)